Journal of The Electrochemical Society

The Multifaceted Role of Boric Acid in Nickel Electrodeposition and Electroforming

To cite this article: C. Enowmbi Tambe *et al* 2024 *J. Electrochem. Soc.* **171** 102503

Journal of The Electrochemical Society, 2024 **171** 102503

The Multifaceted Role of Boric Acid in Nickel Electrodeposition and Electroforming

C. Enowmbi Tambe, T. A. Green,[z] and S. Roy

Department of Chemical and Process Engineering, University of Strathclyde, Glasgow, Scotland G1 1XJ, United Kingdom

This study involved an investigation of the role of boric acid in nickel electroforming from sulfamate electrolytes, especially in relation to its ability to minimise interfacial pH changes during electrodeposition. Initial speciation calculations indicated that buffering by polyborate species and nickel-borate complexes are most likely responsible for this effect. However, the concentration of nickel-borate complexes was too low even at elevated pH to be a significant electroactive species. Polarisation and electrochemical quartz crystal microbalance measurements indicated that, in the absence of boric acid, electrodeposits typically contained $Ni(OH)_2$, while boric acid additions resulted in pure Ni being deposited with a current efficiency approaching unity. Boric acid additions substantially modified the nickel and hydrogen partial currents, and influenced the overall current efficiency. Studies in nickel-free solutions indicated that boric acid adsorbs on the surface which explains the suppression of H_2O reduction observed in the electroforming experiments. Collectively, solution buffering due to polyborate and nickel-borate species and inhibition of H_2O reduction by adsorbed boric acid minimised interfacial pH changes and prevented the formation of nickel hydroxide.

 [DOI: 10.1149/1945-7111/ad80d3]

Manuscript submitted August 6, 2024; revised manuscript received September 25, 2024. Published October 8, 2024.

Supplementary material for this article is available online

Boric acid is an important material in surface finishing and is widely used as an additive for the electrodeposition of iron group (i.e. Fe, Co and Ni) metals and alloys.[1,2] In the case of nickel deposition, boric acid is a key component for formulating sulfate, chloride and sulfamate electrolytes. While boric acid is currently classified as a substance of very high concern (SVHC) under REACH regulations,[3,4] leading to attempts to identify suitable alternatives, its industrial use in surface finishing is still widespread.[2] The function of boric acid in nickel plating is wide-ranging in that it can improve the current efficiency, prevent oxide/hydroxide formation, extend the usable current density range for deposition, and enhance the deposit appearance.[5–8] Boric acid also has important influences on deposit properties such as grain size,[7,9] texture,[8,10] yield strength[9] and internal stress,[6,11] which are key attributes of an electroplated or electroformed product.

The influence of boric acid on nickel deposition have been investigated by many researchers, and these studies have indicated that its primary role is to act as a buffer, thereby controlling the interfacial pH and preventing the formation and precipitation of metal hydroxides on the surface. However, there is no firmly accepted mechanism for the action of boric acid and some of these propositions contradict one another. For example, it has been variously proposed that boric acid functions as a traditional buffer,[12] a complexing agent,[13–16] an adsorbed species which inhibits electrochemical reactions,[17] a proton donor[18] or some combination of these. Given that any replacement for boric acid would need to have similar functionality, it is important to elucidate its exact role in existing electrodeposition processes. Alternatives such as carboxylic acids could be used to buffer such systems,[19,20] but it is not clear if they could fulfil the other important roles ascribed to boric acid such as complexation and surface adsorption/inhibition, and in some cases inferior deposit characteristics were reported in boric acid free systems.[21]

The ability of boric acid to control the interfacial pH during the electrodeposition of pure Ni and Ni alloys has been clearly demonstrated in a number of studies[5,6,11,22,23] using in situ pH probes. These studies employed chloride[5,22,23] or sulfamate electrolytes,[6,11] and demonstrated that the normal interfacial pH increase due to the hydrogen evolution reaction (HER) was significantly reduced at all current densities when boric acid was present. This buffering effect prevented the formation of insoluble $Ni(OH)_2$ on the surface and its subsequent incorporation into the deposit. However, while this interfacial buffering effect has been established experimentally, the mechanism by which this is achieved is still highly contentious. Over the years many hypotheses have been proposed and, due to their importance to the current study, they will be briefly reviewed below.

The original hypothesis was that boric acid acted as a conventional pH buffer.[12] Boric acid is a weak monobasic acid and acts exclusively by acceptance of hydroxyl species rather than as a proton donor:

$$B(OH)_3 + H_2O \Leftrightarrow B(OH)_4^- + H^+ \quad [1]$$

However, given that for this equilibrium, $pK_a = 9.24$, and the practical range of buffering action is typically $pK_a \pm 1$ pH unit, it seems unlikely that it would buffer nickel plating solutions which typically operate under acidic conditions (i.e. $2 < pH < 4$). At high boric acid concentrations and at a more neutral pH, various polyborate species can also form and it has been suggested that the acid-base equilibria associated with the formation of these species may perform a buffering action.[12,17,23,24] For example, the triborate species, $B_3O_3(OH)_4^-$, has a $pK_a \approx 7$ and can therefore buffer solutions in the range $6 < pH < 8$. Owing to their importance, the concentration of polyborates in nickel plating baths has also been assessed[25] by calculating their species distribution as a function of pH, based on their known equilibrium constants.[26,27] The existence of these species has since been confirmed by Raman spectroscopy,[24,28] but there are conflicting views about whether such species are important in nickel plating, especially under acidic conditions.[25]

These inconsistencies led others[13,14] to suggest that buffering action was due to the formation of nickel-borate complexes, as the buffer capacity of boric acid solutions were enhanced in the presence of nickel ions. Tilak[14] suggested that a weak nickel diborate complex was responsible for buffering, and inferred its stability constant from an analysis of titration data performed in the pH range of 5.0–6.5. Note that the formation of polyborate species was not considered in this model, although one would expect there to be significant concentrations of these in this pH range. Despite this omission, the proposition is still valid, however, other studies[29,30] have shown that

[z]E-mail: todd.green@strath.ac.uk

predominantly nickel monoborate complexes are formed, whilst a more recent report[31] suggests that a nickel triborate species is dominant. Given the uncertain and contradictory nature of this data, it has been difficult to incorporate such nickel borate species into deposition and speciation models and quantify their contribution to pH buffering. For this reason, the majority of modelling studies have ignored the possible importance of nickel borate complexes.

In an experimental study, Hoare[15,16] showed that boric acid accelerated the rate of nickel deposition from a Watts bath relative to hydrogen evolution. It was suggested that the nickel-diborate complex proposed by Tilak can be discharged more easily (at a lower overpotentials) than uncomplexed nickel, and this results in reduced hydrogen evolution and a negligible rise in interfacial pH. This model was partially supported by an EQCM study of nickel deposition from a sulfamate bath,[32] and Rigsby[24] also noted that the partial current of cobalt deposition (but not hydrogen) from a sulfate electrolyte was enhanced by boric acid. However, it is not clear that this complex would be present at sufficiently high concentrations to compete with the direct reduction of uncomplexed nickel ions, or necessarily have faster kinetics.[32] In fact, the results of Tsuru[5] obtained from a Watts bath contradict this mechanism in that the partial currents for nickel were not significantly affected by boric acid additions.

An alternative explanation is the blocking/adsorption model proposed by Horkans,[17] where it was suggested that boric acid adsorbs on the surface and inhibits hydrogen evolution. This suppression of the HER results in a reduced rise in the interfacial pH during metal deposition. In studies of the HER from acid sulfate and chloride electrolytes containing no metal ions, it was noted that the limiting current for the reduction of H^+ ions decreased with boric acid concentration, suggesting that it blocks active sites and decreases the active surface area. However, at currents exceeding the limiting value, H_2O reduction occurs and the overpotential for this reaction was significantly reduced by boric acid additions. It is also important to note that boric acid adsorption was only observed in sulfate and not chloride containing solutions, which likely explains why this effect was not observed earlier by Hoare in a Watts bath. The suppression of the H^+ reduction reaction due to surface site blocking, and the apparent depolarisation of H_2O reduction was subsequently noted in other studies.[18,23,24,33]

A more recent study[18] by Zech and Landolt proposed a model where the pH was not controlled by the traditional buffering action of monoborate or polyborate species, but the dissociation of these species at the interface could prevent large pH changes. In effect, their model showed that a rise in interfacial pH causes monoborate and polyborate species to dissociate and supply additional protons into the diffusion layer so that proton reduction is extended to more negative potentials and higher current densities. This effect minimises the pH changes at the cathode surface associated with the transition to H_2O reduction. This mechanism is plausible but, as noted by Horkans,[17] it requires that the dissociation rate of borate species to be sufficiently fast to act as effective proton donors. Importantly, the authors attribute the apparent enhancement of the H_2O reduction current with boric acid noted in their own study and by others[23,24,33] to this dissociation effect. They also presented experimental data which indicated suppression of the HER involving H^+ reduction due to boric acid adsorption, corresponding to the earlier suggestion of Horkans.[17]

Despite more than 50 years of study, the role of boric acid in nickel electroplating baths is still unclear. All the models proposed so far all have limitations and none appear capable of explaining or rationalising all experimental findings. As such, the present work attempts to clarify and address some of these issues by combining a speciation analysis of the plating solutions with electrochemical measurements. The main role of the speciation study is to understand the relative importance of different solution species including monoborate, polyborate and nickel-borate complexes. This can then be used to assist in interpreting the results of the electrochemical study. The primary tool of the electrochemical investigation is the EQCM which is capable of measuring the overall current efficiency, partial currents, surface adsorption of species, and discriminating between the deposition of metals and oxide/hydroxides.

The main objective of this study is to examine the influence of boric acid on the deposition of nickel from sulfamate electrolytes that are used in commercial electroforming applications.[34–37] As noted earlier, boric acid is critical for producing electroforms with the required properties, and its continued use (or mandated replacement) requires a better understanding of its multifunction role. While the majority of earlier studies have focussed on sulfate, chloride, and chloride-sulfate electrolytes, the role of boric acid in relation to sulfamate electrolytes remains relatively unexplored. Another key objective is to interpret the results in terms of the four models proposed, and make some assessment of their validity and relevance in nickel electroforming.

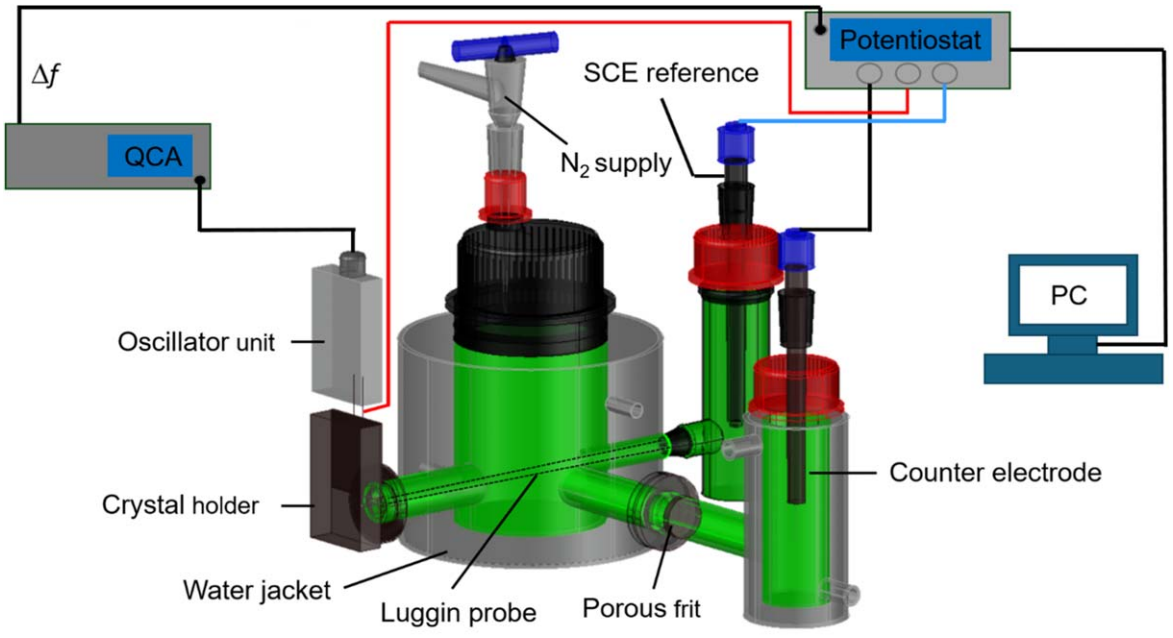

Figure 1. Schematic diagram of the electrochemical cell used in the EQCM experiments.

Experimental and Modelling Methods

Solutions.—All electrolyte solutions were prepared with analytical (AR) grade chemicals and 18.2 MΩ cm ultrapure water. Nickel sulfamate tetrahydrate ($Ni(SO_3NH_2)_2.4H_2O$), >98%) and boric acid ($B(OH)_3$, >99.5%) were obtained from Sigma-Aldrich and used as received. The base electrolyte contained 1.785 M nickel sulfamate, while the boric acid containing solution contained 0.49 M, 0.65 M or 0.81 M $B(OH)_3$ with a resulting pH = 3.2 ± 0.2. These were formulated to yield compositions which closely resembled those used in commercial nickel electroforming processes and also to investigate the effect of boric acid additions. Some additional experiments were performed in potassium sulfamate (KSO_3NH_2, 98% Alfa Aesar) acid to study the adsorption of borate species without interference from nickel deposition. The composition of this electrolyte was 3.57 M KSO_3NH_2 (to ensure the same total sulfamate ion concentration) and 0.65 M $B(OH)_3$.

EQCM experiments.—A jacketed, glass electrochemical cell with a volume of 100 ml was used in the EQCM experiments and is shown schematically in Fig. 1.[38] A thermostatic bath was used to pump water through the jacket so the cell could be maintained at a temperature of 45 °C. The counter electrode was a platinum wire and was separated from the main compartment of the cell by a porous glass frit. This prevented anode products from influencing the deposition process.[39] The reference electrode was a standard calomel electrode (SCE) and this was placed in a Luggin capillary whose tip was located 7 mm from the surface of the working electrode. In this manner, the effects of *IR* drop in the solution were minimised. Before each experiment, the main compartment of the cell could be sparged with high purity N_2 to remove dissolved oxygen, and a flow of N_2 was maintained in the headspace during measurements.

The working electrode (WE) comprised a metallised quartz crystal, mounted in a crystal holder that attached to the main cell compartment. When assembled and mounted, the active area of the WE was 0.196 cm^2. The commercially sourced quartz crystals (Seiko EG&G Ltd) were unpolished AT-cut disks with a resonant frequency 9 MHz. These were sputter-coated with a layer of 304-grade stainless steel (SS) or gold. The former material was chosen as it typically used for the mandrel (substrate) in electroforming[34,36,37] but note that due to the nature of the sputtering process its composition may differ slightly from bulk 304 SS material. The crystals could be reused after each experiment by dissolving the nickel deposits in 0.1 M HNO_3. Dilute nitric acid was used to avoid passivating the 304 SS. Nickel substrates were also prepared by electrodepositing (at 5 mA cm^{-2} for 300 s) a 0.5 μm layer on to Au crystals from a solution containing 1.785 M $Ni(SO_3NH_2)_2$ and 0.65 M $B(OH)_3$.

The change in the resonant frequency, Δf, of the quartz crystals was measured using an analyser (QCM 922 A, Seiko EG&G Ltd). This frequency change was converted to a proportional voltage and this was measured using the analogue input channel on the potentiostat. The 304 SS quartz crystal was calibrated by depositing nickel from a sulfamate solution containing 1.785 M $Ni(SO_3NH_2)_2$ and 0.49 M $B(OH)_3$. These depositions were performed galvanostatically at 2 mA cm^{-2} for 1500 s. Under these conditions, nickel could be plated with a low roughness, low stress and with a current efficiency close to unity. The calibration factor was determined to be 0.906 Hz ng^{-1} for the 304 SS coated quartz crystal.

Polarisation experiments were performed using a potentiostat (PGSTAT101, Metrohm Autolab) in a conventional three-electrode configuration and using the Nova 2.1 software for data collection and analysis. In a typical experiment, a linear potential scan was performed starting from the open circuit potential (∼+0.2 V) to −1.7 V vs SCE at a scan rate of 5 mV s^{-1}. During the potentiodynamic scan, the frequency of the quartz crystal was monitored simultaneously to assess any mass changes on the electrode surface. For each experiment, after assembling and filling the cell, the solution was degassed and the quartz crystal was allowed to stabilise for another 15 min until the frequency change was less than 1 Hz min^{-1}. Following this initial stabilisation period, the polarisation scan was initiated.

Speciation modelling.—Prior to the electrochemical measurements being performed, a speciation analysis of the sulfamate electrolyte was undertaken to identify the dominant borate and nickel species as a function of pH. This approach was used to discriminate between some of the proposed models for the role of boric acid, and also assist in interpreting the experimental results. In particular, nickel-borate complexes were included in the model so as to assess their importance in terms of their buffering ability and as electroactive species, as were various polyborate species. The overall boron speciation is quite complex, and is summarised in Fig. 2. The equilibrium concentrations of various nickel and borate complexes were calculated using the MINEQL+ v5.0 modelling software. This is a general-purpose program for solving complex chemical equilibria in aqueous systems, and employs the Newton-

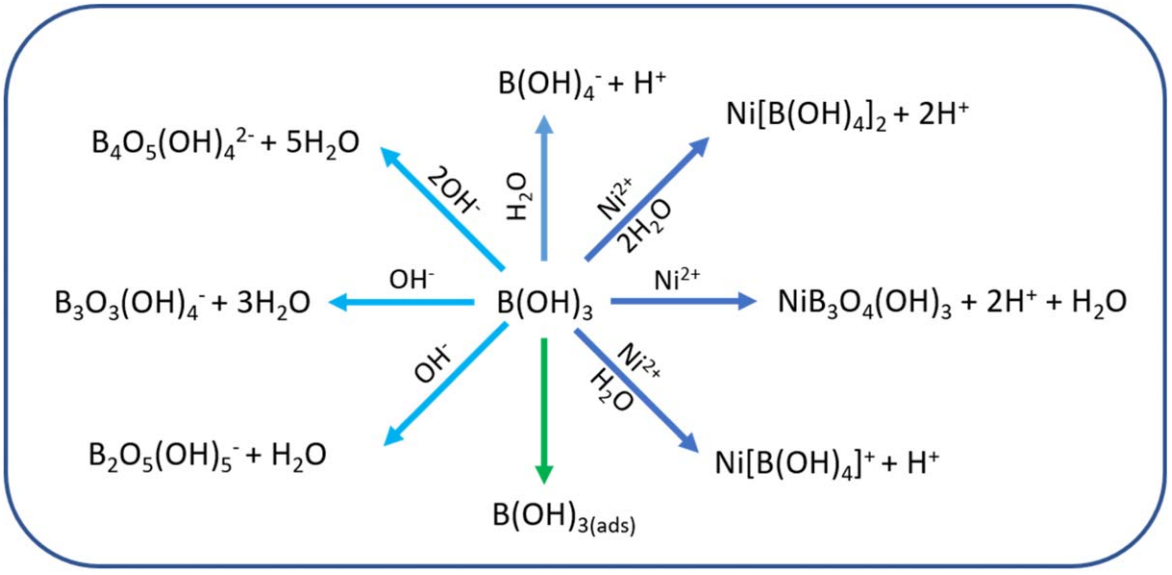

Figure 2. Schematic diagram of the solution chemistry for boric acid showing the formation of borates, polyborates, nickel-borate complexes and the possibility of surface adsorption.

Rhapson method to solve iteratively the mass balance equations associated with each metal ion and ligand. As well as modelling dissolved species, the program also considers the possible precipitation of various insoluble species. The overall approach employed was similar to that used previously for analysing speciation in the Cu-Ni citrate[40,41] and Au sulfite-thiosulfate[42] systems.

While MINEQL+ has an internal database of equilibrium constants and other thermodynamic data for various species, it was necessary to supplement this with additional data for borate species (Table I). Note that while the stability constants for mono and polyborate species are well established,[26,27] those for nickel borate complexes are more uncertain. Various monoborate,[30] diborate[14,29] and triborate[31] nickel complexes have been proposed, and concerns have been raised[43,44] about the reliability of some of this data. Notably, none of these studies meets the criteria for inclusion in the NIST Critical Stability Constant Database,[45] but some are included in non-critical databases (JESS[44] and SC-Database[46]). The speciation model only considered nickel-borate complexes whose stability constants were judged reliable and consistent with other data sets.

It was also assumed that sulfamate ions do not complex with nickel ions and this supposition is supported by some previous studies,[47] but the equilibrium between the sulfamate ion and sulfamic acid ($pK_a = 1.05$) was considered. Due to a lack of available data for some species it was not possible to correct for temperature effects, and all calculations were performed at 25 °C compared to an experimental temperature of 45 °C. Previous work[48] has already demonstrated that the overall borate speciation does not change substantially over the temperature range 25–70 °C. The MINEQL+ model is generally used for dilute solutions where the equivalence between concentrations and activities of species can be justified. For more concentrated solutions, the program can apply the Davies equation to correct the stability constants for activity effects. However, this correction is only valid for $I < 0.5$ and, because the ionic strength of the nickel solutions was typically $I > 5.0$, this approach was not feasible. Due to the difficulty in rigorously correcting for activity effects, earlier speciation modelling studies[10,18,25,33,49] have employed concentrations, and this is the approach adopted in the present study.

Results and Discussion

Speciation analysis.—Calculations of the borate speciation were initially performed for an electrolyte containing 1.8 M $Ni(SO_3NH_2)_2$ and 0.50 M $B(OH)_3$ and initially assuming that Ni-borate complexes do not form. The distribution of borate species as a function of pH is shown in Fig. 3. This clearly shows that under acidic and neutral conditions the dominant species is boric acid, $B(OH)_3$, while under alkaline conditions it is the borate anion, $B(OH)_4^-$. In the intermediate region ($5 < pH < 12$) various polyborate species are significant, especially the triborate $B_3O_3(OH)_4^-$ and tetraborate $B_4O_5(OH)_4^-$ species. Additional calculations (Figs. S1 and S2) indicate that polyborate are typically negligible species at $[B(OH)_3] < 0.1$ M but are increasingly important for $[B(OH)_3] > 0.5$ M. These findings are in good agreement with previous speciation[25,31] and Raman studies[24,28] performed in chloride and sulfate electrolytes.

The more complex acid-base equilibria associated with polyborates (Table I) has been used to explain[12,17,23,24] apparent buffering action when the pH is well below the pK_a of the monoborate species. Figure 3 indicates that the dominant polyborate species, $B_3O_3(OH)_4^-$ ($pK_a = 7.0$) has a significant concentration for $pH > 5.5$ and could therefore buffer the solution according to the following equilibrium:

$$3B(OH)_3 \Leftrightarrow B_3O_3(OH)_4^- + 2H_2O + H^+ \quad [2]$$

Buffer capacity is limited by the relatively low concentration of the triborate species, but this is increased at higher boric acid concentrations and pH. A number of authors[17,50,51] have proposed that the triborate species, $B_3O_3(OH)_4^-$, is a likely buffering agent for nickel and cobalt plating from sulfate and chloride electrolytes. In the study of Rigsby[24] it was shown by titration analysis of a 0.65 M boric acid solution that the various polyborate equilibrium contribute to produce an apparent $pK_a \approx 6.5$, which is consistent with $B_3O_3(OH)_4^-$ being the dominant buffering species.

Of more significance is the possible role of various nickel-borate complexes, and Fig. 4 shows the concentration of complexed and uncomplexed borate species as a function of pH in a solution containing 1.8 M $Ni(SO_3NH_2)_2$ and 0.50 M $B(OH)_3$. In this example, it has been assumed that the complex is nickel diborate, $Ni[B(OH)_4]_2$, as proposed by Tilak.[14] The figure clearly shows that the this complex only has a significant concentration in the range of pH = 6–8, and uncomplexed borate and polyborates are still the dominant species. Similar trends in speciation were obtained with the assumption that either nickel monoborate,[30] $Ni[B(OH)_4]^+$, or triborate,[31] $NiB_3O_4(OH)_3$, complexes are formed (Figs. S3 and S4).

Note that the observed decline in the $Ni[B(OH)_4]_2$ concentration at $pH > 6.2$ arises due to the precipitation of $Ni(OH)_2$. This removes essentially all Ni^{2+} ions from solution and therefore there are discontinuities in the concentration profiles of all Ni species around a pH = 6 (e.g. Figures 4, 5, S3 and S4). Similar discontinuities were reported in other systems[33,52] when the possibility of $Ni(OH)_2$ precipitation was considered. While removing these precipitating species from the model would result in more continuous concentration profiles, this would not reflect the realities of the actual system, which does undergo precipitation at pH ≈ 6.

These results indicate that these nickel borate complexes compete with the formation of polyborate species for $5.5 < pH < 8.0$ and, as proposed earlier,[13,14] they could also function as buffers. For example, in the case of the nickel monoborate, diborate and triborate

Table I. Summary of thermodynamic data (overall stability constant, β) for various borate species used in the speciation model. Note that some equilibria are defined with respect to $B(OH)_3$ and others to the $B(OH)_4^-$ species. Additionally, in some sources[14,43] the monoborate anion is written as $H_2BO_3^-$ or BO_2^-, but $B(OH)_4^-$ is the most accurate representation of its structure. Values of log β marked with * are considered to have low reliability. These are included for completion, but were not used in any of the speciation models.

Borate equilibria	log β	Ionic Strength I	Temperature °C	References
$Ni^{2+} + B(OH)_4^- \Leftrightarrow NiB(OH)_4^+$	1.63	0	25	30
$Ni^{2+} + B(OH)_4^- \Leftrightarrow NiB(OH)_4^+$	2.17	0.1	25	29
$Ni^{2+} + 2B(OH)_4^- \Leftrightarrow Ni[B(OH)_4]_2$	4.9	5.8	55	14
$Ni^{2+} + 3B(OH)_3 \Leftrightarrow NiB_3O_4(OH)_3 + 2H^+ + H_2O$	−11.5	0	25	31
$Ni^{2+} + 3B(OH)_4^- \Leftrightarrow Ni[B(OH)_4]_3^-$	8.2*	0	25	44
$Ni^{2+} + 3BO_2^- \Leftrightarrow Ni(BO_2)_3^-$	8.54*	0	22	43
$B(OH)_3 + H_2O \Leftrightarrow B(OH)_4^- + H^+$	9.24	0	25	26, 27
$2B(OH)_3 + OH^- \Leftrightarrow B_2O_5(OH)_5^- + H_2O$	4.69	0	25	26, 27
$3B(OH)_3 + OH^- \Leftrightarrow B_3O_3(OH)_4^- + 3H_2O$	6.69	0	25	26, 27
$4B(OH)_3 + 2OH^- \Leftrightarrow B_4O_5(OH)_4^{2-} + 5H_2O$	12.94	0	25	26, 27

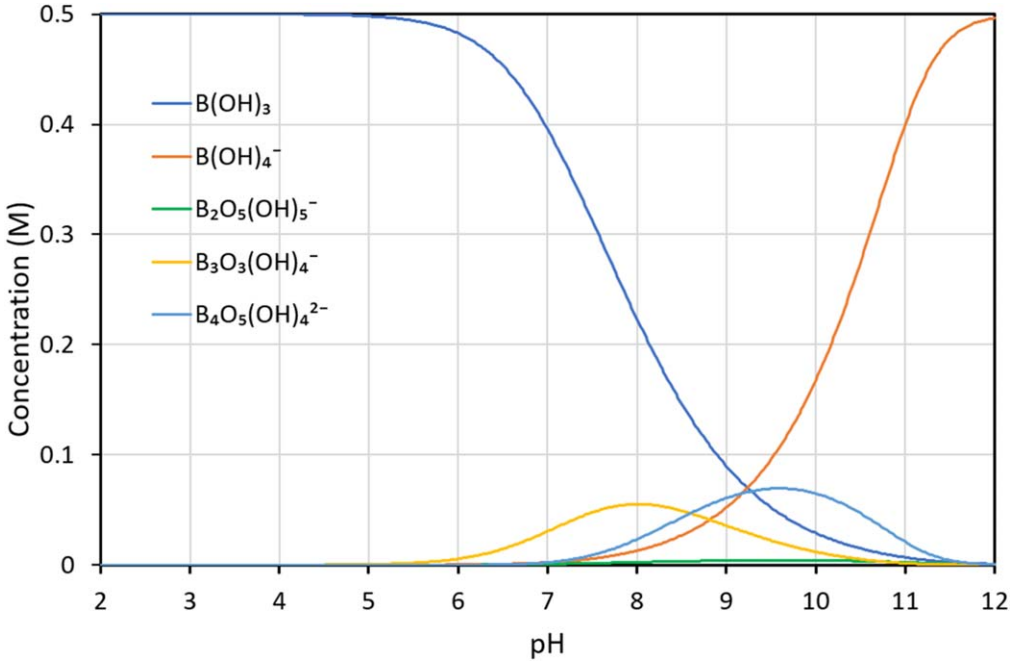

Figure 3. Distribution of various borate and polyborate species as a function of pH in a solution containing 1.8 M $Ni(SO_3NH_2)_2$ and 0.50 M $B(OH)_3$ with the assumption that Ni-borate complexes do not form.

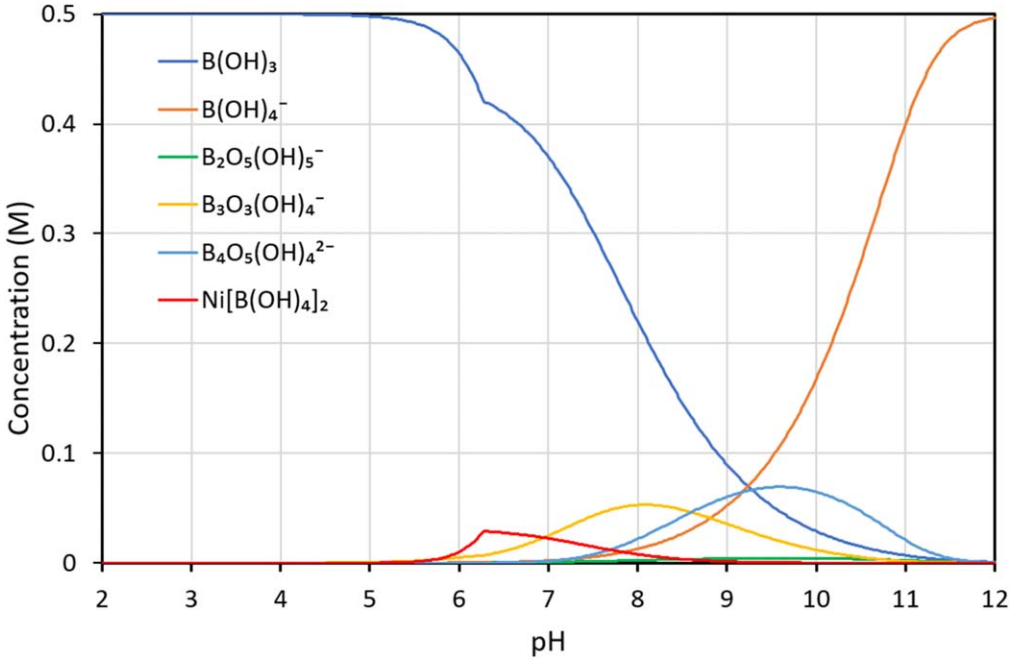

Figure 4. Distribution of various borate and polyborate species as a function of pH in a solution containing 1.8 M $Ni(SO_3NH_2)_2$ and 0.50 M $B(OH)_3$ assuming the $Ni[B(OH)_4]_2$ complex forms.

complexes the following equilibrium could provide buffering:

$$Ni^{2+} + B(OH)_3 + H_2O \Leftrightarrow Ni[B(OH)_4]^+ + H^+ \quad [3]$$

$$Ni^{2+} + 2B(OH)_3 + 2H_2O \Leftrightarrow Ni[B(OH)_4]_2 + 2H^+ \quad [4]$$

$$Ni^{2+} + 3B(OH)_3 \Leftrightarrow NiB_3O_4(OH)_3 + 2H^+ + H_2O \quad [5]$$

It is not possible to identify from the speciation analysis exactly what species are providing buffering, but clearly the triborate species and nickel borate complexes are all plausible candidates. Importantly, previous observations[13,14,22] that nickel ions increase the buffer capacity of boric acid solutions indicate that nickel borate complexes must contribute to some extent. As well as acting as conventional buffers, these species may also act as proton donors and this is the basis of the model proposed by Zech[18] for minimising interfacial pH increases.

It is also instructive to examine the speciation in terms of the nickel component, and this is illustrated in Fig. 5. As well as the $Ni[B(OH)_4]_2$ species and Ni^{2+}, the figure also shows the equilibrium concentrations of various hydrolysed nickel species such as Ni^{2+}, $NiOH^+$, $Ni(OH)_{2(aq)}$, and $Ni(OH)_3^-$ and $Ni(OH)_2$. Figure 4 indicates

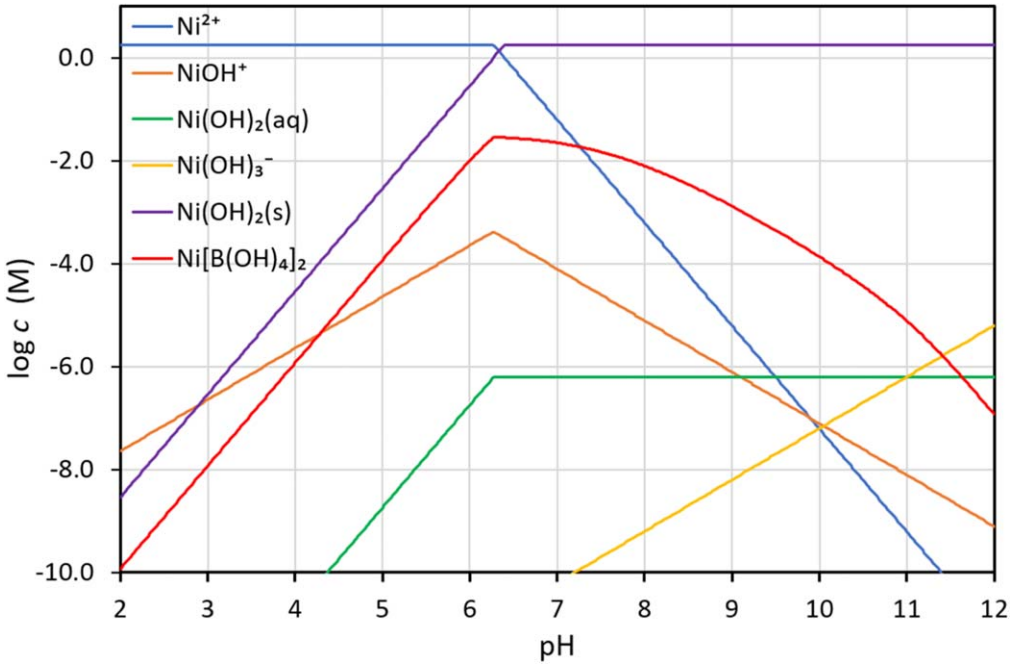

Figure 5. Concentration profiles of various nickel species as a function of pH in a solution containing 1.8 M $Ni(SO_3NH_2)_2$ and 0.50 M $B(OH)_3$ assuming the $Ni[B(OH)_4]_2$ complex forms. The model predicts that $Ni(OH)_2$ precipitates at pH = 6.2.

that the dominant nickel species is Ni^{2+} up until the precipitation of $Ni(OH)_2$ at pH = 6.2, with the nickel diborate complex being a minority components at all pHs. Note that hydrolysed species such as $Ni(OH)_{2(aq)}$ and $NiOH^+$ has also been suggested[6,23,51] to be precursors to Ni deposition, but Fig. 5 shows that they are also present at very low concentrations. Earlier experimental studies[6] and thermodynamic[52] modelling of nickel sulfamate electrolytes with similar compositions to this study also confirmed that $Ni(OH)_2$ precipitation occurs at pH ≈ 6. This is also consistent with the known solubility product of $Ni(OH)_2$ ($pK_{sp} = -15.3$) and with $[Ni^{2+}] = 1.8$ M.

The relatively low concentration of nickel borate complexes compared to uncomplexed Ni^{2+} is indicated in Fig. 6 which plots the concentration of the $Ni[B(OH)_4]^+$, $Ni[B(OH)_4]_2$ and $NiB_3O_4(OH)_3$, as a function of pH. Note that these represent independent calculations, plotted on the same graph to facilitate comparison, and Fig. 6 does not imply that the complexes co-exist. Under strongly acidic conditions they all have extremely low concentrations but these increase rapidly with pH. However, at the typical operating conditions of nickel sulfamate bath (pH ≈ 3–4) they have concentrations of 10^{-4} to 10^{-6} M. This makes it difficult to justify that nickel deposition occurs mainly by direct electroreduction of a complex, as proposed by Hoare. Only at pH ≈ 6 do their concentrations become significant and for the strongest complex, $NiB_3O_4(OH)_3$, approaches 10^{-1} M. However, this is still only 5% of the uncomplexed Ni^{2+} concentration. For pH > 6 their concentrations plateau or decline due to the precipitation of $Ni(OH)_2$. In the absence of precipitation, the complexes would become the dominant Ni species at pH = 7, but this condition cannot be realised experimentally. There is little comparable speciation data, but two earlier studies[49,52] (albeit on different electrolyte systems and with different assumption regarding complexation) also suggest that nickel borate species only have appreciable concentrations under near-neutral conditions.

These preliminary speciation calculations have indicated the following main points. Firstly, polyborate species and nickel-borate complexes do become significant species for pH > 5.5 and may contribute to buffering action either by their associated acid-base equilibria or possibly by acting as proton donors. At the normal operating point of sulfamate baths (pH ≈ 3–4) their concentrations are relatively low ($<10^{-4}$ M), but as the interfacial pH rises during electrodeposition these will increase to between 10^{-2} and 10^{-1} M and they can then provide significant buffering capacity. However, the concentration of nickel borate complexes will be too low even at the point where the solution starts to precipitate (pH = 6.2) for them to be significant electroactive species. It may still be possible that boric acid facilitates nickel deposition, but this is clearly not through the formation of nickel-borate complexes.

Experimental EQCM study.—Initial voltammetric and EQCM studies were performed on a solution which contained 1.78 M $Ni(SO_3NH_2)_2$ and no added boric acid. Figure 7 shows the resulting polarisation data for a 304 SS quartz crystal electrode obtained by scanning from the OCP to −1.2 V vs SCE, along with the measured change, Δf. The measured current, j_{meas}, is plotted along with the calculated partial current for Ni deposition, j_{Ni}. This was calculated using the Faraday and Sauerbrey equations, using the calibration factor determined previously. Initially there is relatively good agreement between j_{meas} and the calculated j_{Ni} indicating that only Ni is being deposited and with a current efficiency approaching unity. However, at more negative potentials the measured j_{Ni} is higher than the measured current indicating an apparent current efficiency in excess of unity.

The most likely explanation for these results is that the mass gain measured by the EQCM included contributions from both Ni deposition and from the precipitation of the $Ni(OH)_2$. The overall reactions that occur in system and their estimated reversible potential, E_r, at pH = 3 are given below:

$$Ni^{2+} + 2e - \Leftrightarrow Ni \quad (E_r = -0.48 \text{ V vs SCE}) \qquad [6]$$

$$2H^+ + 2e - \Leftrightarrow H_2 \quad (E_r = -0.42 \text{ V vs SCE}) \qquad [7]$$

$$2H_2O + 2e - \Leftrightarrow H_2 + 2OH^- \quad (E_r = -0.42 \text{ V vs SCE}) \qquad [8]$$

Both hydrogen evolution reactions (HER) are capable of increasing the pH at the interface by either consuming protons or by generating hydroxide ions. Initially, only the reduction of H^+ occurs, but once the limiting current is exceeded (estimated to be 0.20 mA cm^{-2} at pH = 4 and 2.0 mA cm^{-2} at pH = 3) H_2O reduction dominates and finally direct nickel deposition commences. The sequence in which

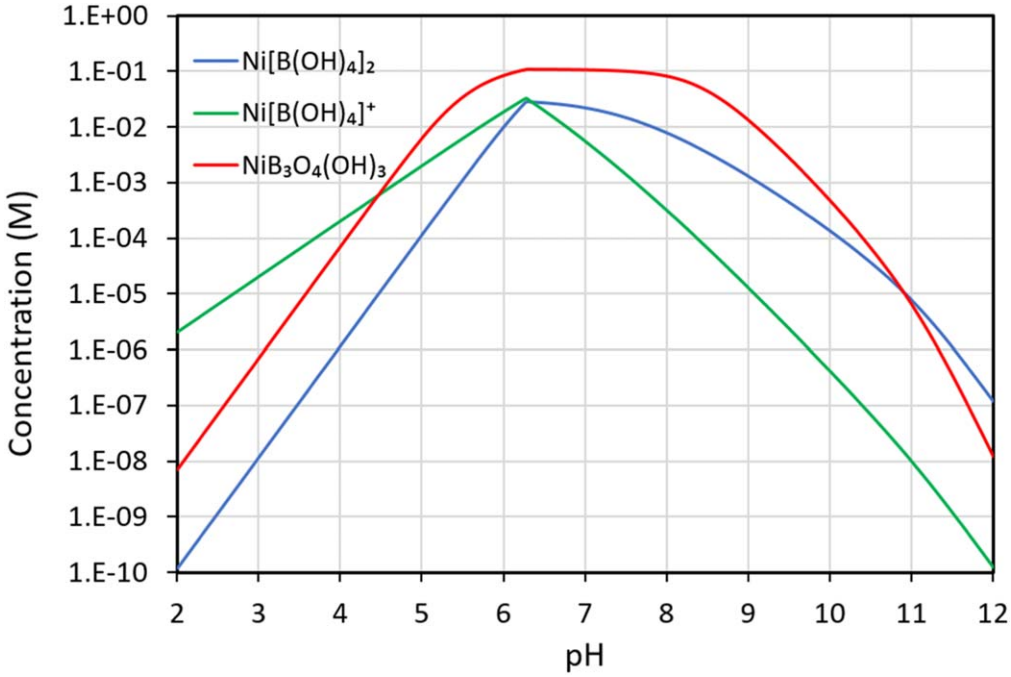

Figure 6. Concentration profiles of the monoborate, $Ni[B(OH)_4]^+$, diborate $Ni[B(OH)_4]_2$ and triborate $NiB_3O_4(OH)_3$ nickel complexes as a function of pH. These profiles represent separate calculations, and the complexes do not coexist. Their concentrations go through a maxima at pH = 6.2 before declining due to the precipitation of $Ni(OH)_2$.

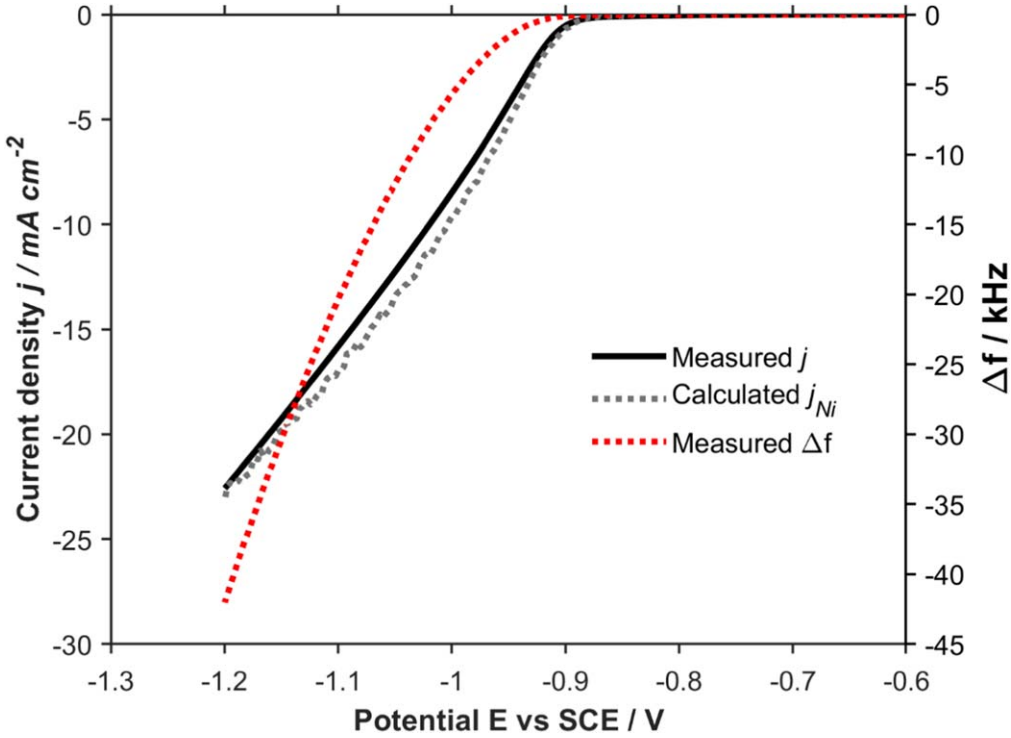

Figure 7. Polarisation scan and EQCM frequency change, Δf, for nickel deposition from a 1.78 M $Ni(SO_3NH_2)_2$ solution containing no added boric acid.

these electrochemical reactions occur has been demonstrated in a number of experimental studies.[53,54] At some point enough OH^- is generated by the HER to exceed the solubility product of $Ni(OH)_2$, leading to its precipitation. The earlier speciation studies suggest that this typically occurs at a pH ≈ 6.

This idea can be examined by generating a plot of the mass change, Δm, measured by the EQCM vs the charge passed, Q, in the polarisation scans. The theoretical slope ($\Delta m/Q$) is 304.16 ng mC^{-1} for Ni deposition and 480.43 ng $mC^{-1}$for $Ni(OH)_2$ formation. The actual slopes calculated from the EQCM data correspond to 336.35 ng mC^{-1} at 45 °C. These data are plotted in Fig. 8, and shows that the observed mass change is consistent with concurrent Ni and $Ni(OH)_2$ deposition. Interestingly, the inset to Fig. 8 which shows the early stages of Ni deposition indicates that $Ni(OH)_2$ is formed almost immediately, when the current density is still very low. The mole fraction, α, of nickel in the deposit can be obtained

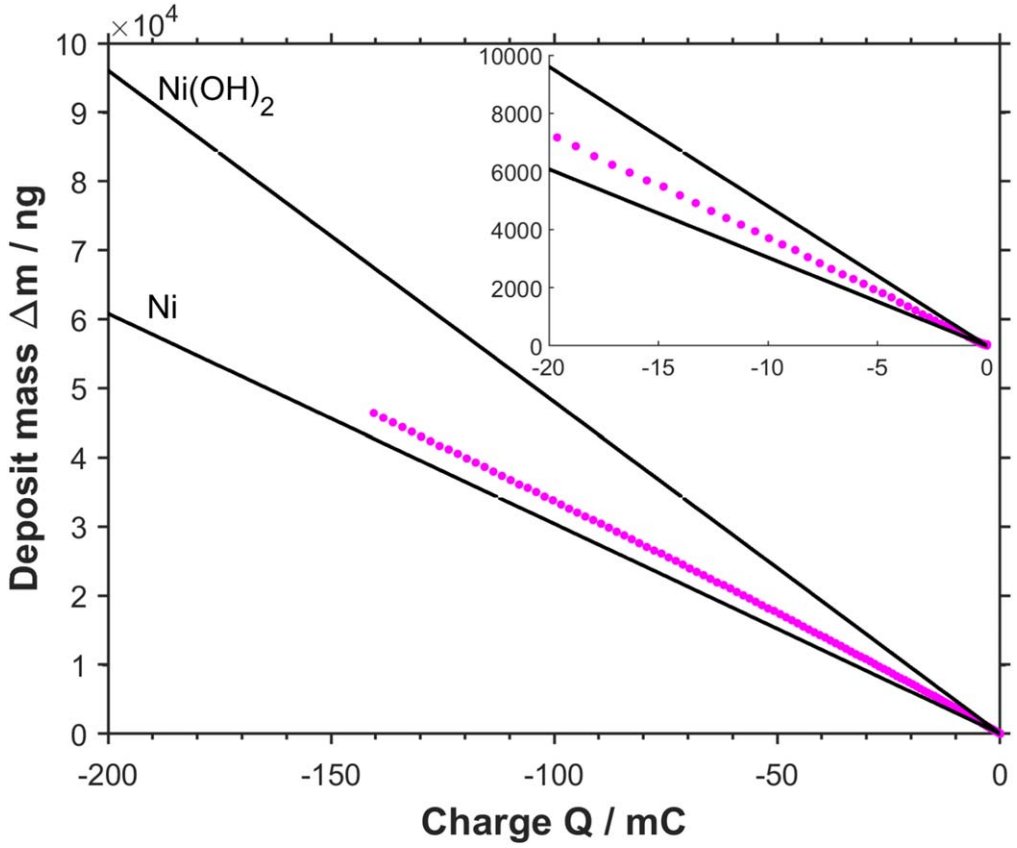

Figure 8. Plot of deposition mass, Δm, vs charge, Q, for nickel deposition from a 1.78 M $Ni(SO_3NH_2)_2$ nickel sulfamate solution containing no boric acid. The theoretical lines for deposition of Ni and $Ni(OH)_2$ are shown.

from the following expression:

$$\Delta m = \alpha \Delta m_{Ni} + (1 - \alpha)\Delta m_{Ni(OH)2} \quad [9]$$

Applying this formula to the data in Fig. 8, a value of $\alpha = 0.81$ is obtained indicating the incorporation of approximately 20 mole% of $Ni(OH)_2$ into the deposit. These results are consistent with some earlier EQCM studies of the deposition of nickel[55,56] and cobalt[57,58] deposition, which typically showed significant amounts of incorporated $Co(OH)_2$ and $Ni(OH)_2$ in the absence of boric acid. These hydroxide inclusions typically have a detrimental effect on deposit properties.[5,6]

Polarisation and EQCM data for solutions containing data 1.78 M $Ni(SO_3NH_2)_2$ and varying amounts of boric acid are shown in Fig. 9. The measured current, j_{meas}, is plotted along with partial current for Ni deposition, j_{Ni}, calculated from the mass change (Δm) measured by the EQCM. In the potential region -0.9 V to -1.1 V vs SCE, higher boric acid concentrations increase the Ni deposition current at a fixed potential, but above -1.1 V the currents are similar. In the presence of boric acid, the partial current j_{Ni} are less than $j_{meas.}$ This indicates that the current efficiency is less than unity, due to the co-evolution of hydrogen. At the highest boric acid concentration (0.81 M) there is an initial region ($E > -0.87$ V) where there is no nickel deposition and mostly the HER is occurring.

The effects of boric acid on the nickel deposition process is illustrated more conveniently in Fig. 10 which is a plot of Δm vs Q. In contrast to the boric acid free solution (Fig. 8) all experimental slopes are lower than the theoretical slope for $Ni(OH)_2$ and Ni deposition. This shows that the presence of boric acid prevents the formation of $Ni(OH)_2$ and pure nickel is deposited at a current efficiency just below unity. This agrees with earlier EQCM studies of nickel[55,56] and cobalt[57,58] deposition from chloride, sulfate and sulfamate solutions. The inset to Fig. 10 shows the initial stages of the deposition process. At the lowest boric acid concentrations, deposition occurs significantly below the Ni theoretical line, and for the highest boric acid concentrations there is an initial period where only the HER occurs.

The influence of boric acid on the current efficiencies for nickel deposition as a function of the current density is captured in Fig. 11. For the highest boric acid concentration, there is a current density range (<2.5 mA cm^{-2}) where the HER dominates and current efficiency is essentially zero. This is also noticeable in the inset region of Fig. 10. However, at higher current densities the boric acid concentration appears to have a relatively minor effect on the current efficiencies, and all baths eventually approach comparable (and high) values. Most previous studies[5–7,23,24] of nickel electrodeposition from chloride, sulfate and sulfamate solutions indicate the current efficiency is slightly improved by boric acid additions. For example, in a nickel sulfamate bath Tsuru[5] reported that, at high current densities, the current efficiency increased only slightly from 0.97 to 0.99 as boric acid concentration was increased from 0.16 M to 0.81 M.

In order to understand the influence of boric acid additions on nickel deposition and the HER, it is useful to extract the partial currents for the nickel (j_{Ni}) and hydrogen reactions ($j_H = j_{meas} - j_{Ni}$) (Fig. 11). Note that it was not possible to perform this analysis for the solution with no added boric acid due to complications arising from the co-deposition of $Ni(OH)_2$. Figure 12 shows that the boric acid additions generally increase the partial current for Ni deposition at a given potential, but this effect becomes less noticeable at high potentials ($E > -1.15$ V). This is consistent with some previous studies[15,16] indicating that boric acid aids nickel deposition, but its influence on the HER also needs to be considered.

The influence of boric acid on the hydrogen partial current is more complex but, in all cases, there is some hydrogen evolution

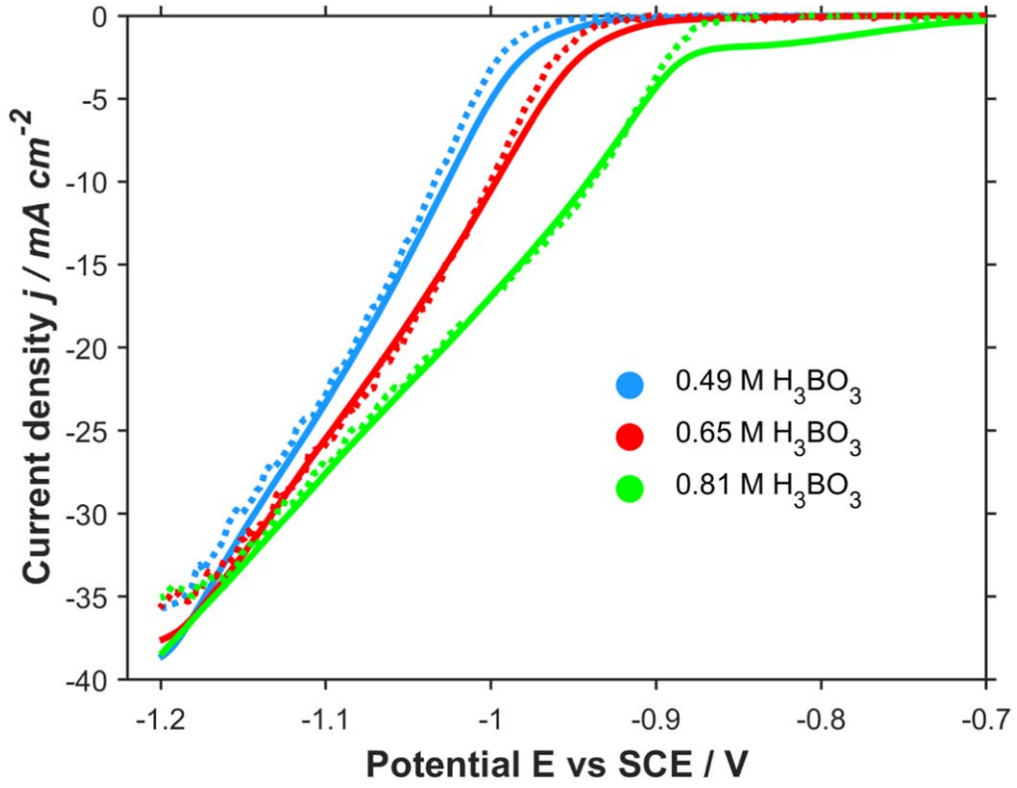

Figure 9. Polarisation scans for nickel deposition from 1.78 M $Ni(SO_3NH_2)_2$ solutions containing 0.49 M $B(OH)_3$, 0.61 M $B(OH)_3$, and 0.81 M $B(OH)_3$. Measured currents, j_{meas}, are solid lines and calculated partial current for Ni, j_{Ni}, are dotted lines.

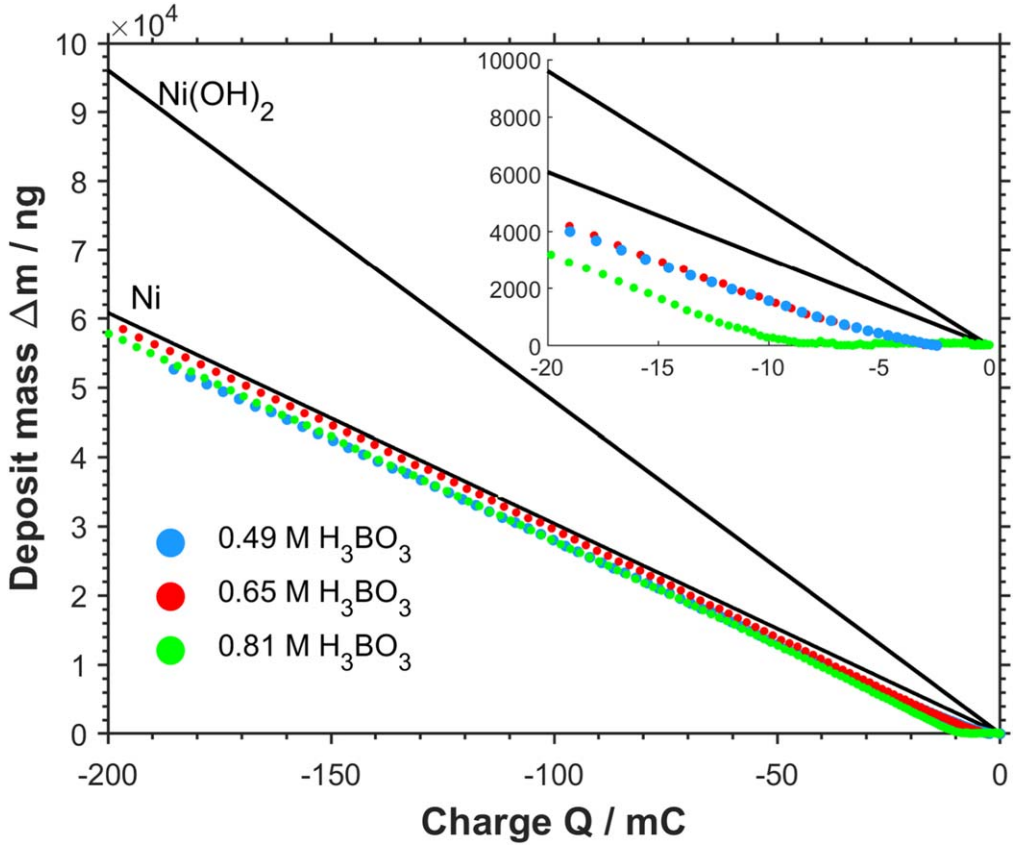

Figure 10. Plot of deposition mass, Δm, vs charge, Q, for nickel deposition from 1.78 M $Ni(SO_3NH_2)_2$ solutions containing 0.49 M $B(OH)_3$, 0.61 M $B(OH)_3$, and 0.81 M $B(OH)_3$. The theoretical lines for deposition of Ni and $Ni(OH)_2$ are shown.

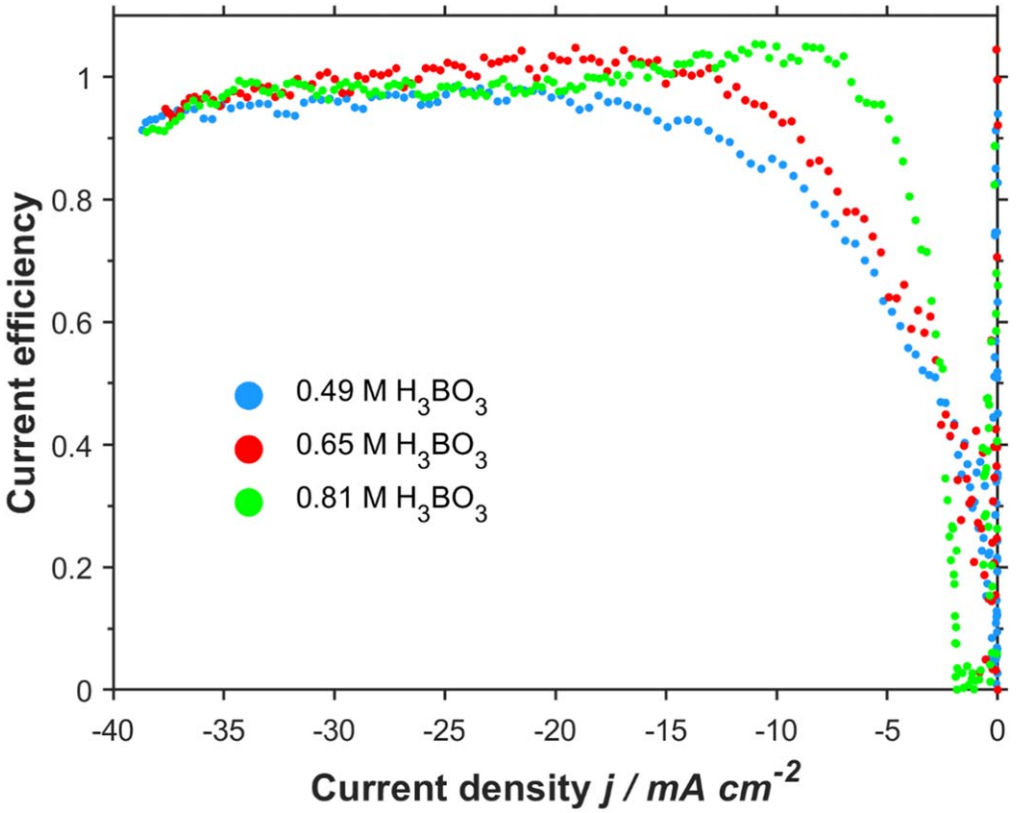

Figure 11. Plot of the current efficiency vs current density at various boric acid concentrations.

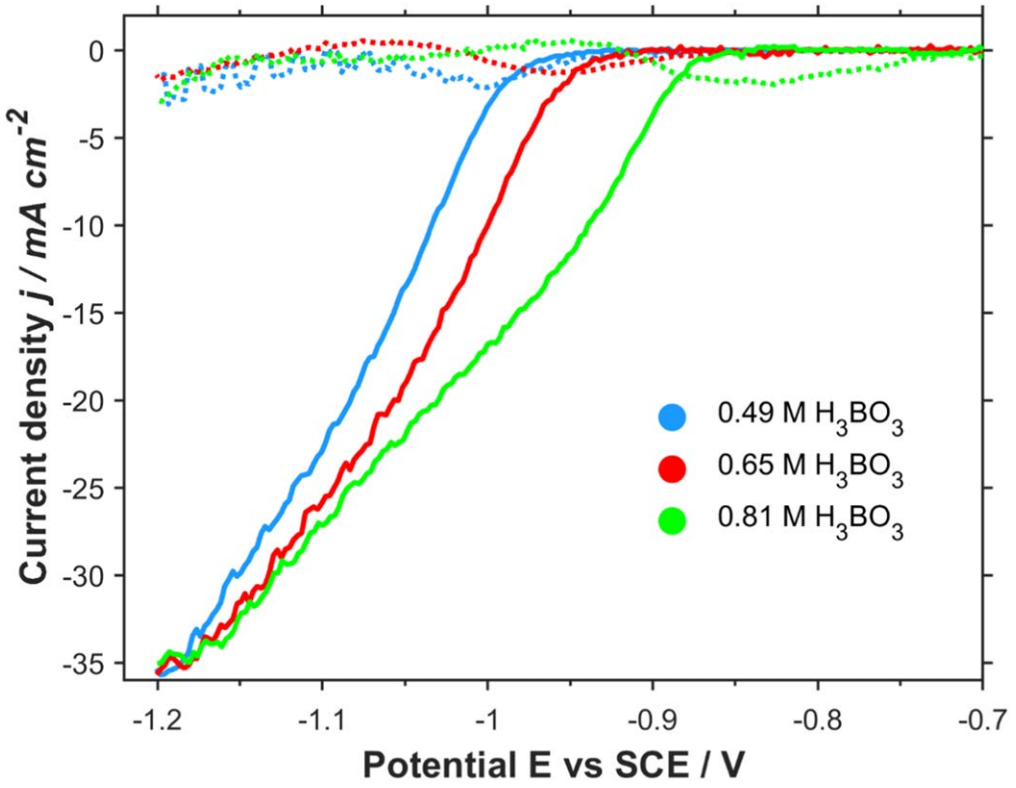

Figure 12. Influence of boric acid additions on the partial current for nickel, j_{Ni}, (solid lines) and hydrogen, j_H, (dotted lines) as a function of potential.

before Ni deposition commences. Up to the limiting current density of $\sim$1 mA cm^{-2} this arises from H^+ reduction, but beyond this the partial current is increasingly due to H_2O reduction. Notably the hydrogen partial current slowly increases but goes through a maximum and then declines, and this coincides with the onset of nickel deposition. The main effect of boric acid is to shift the

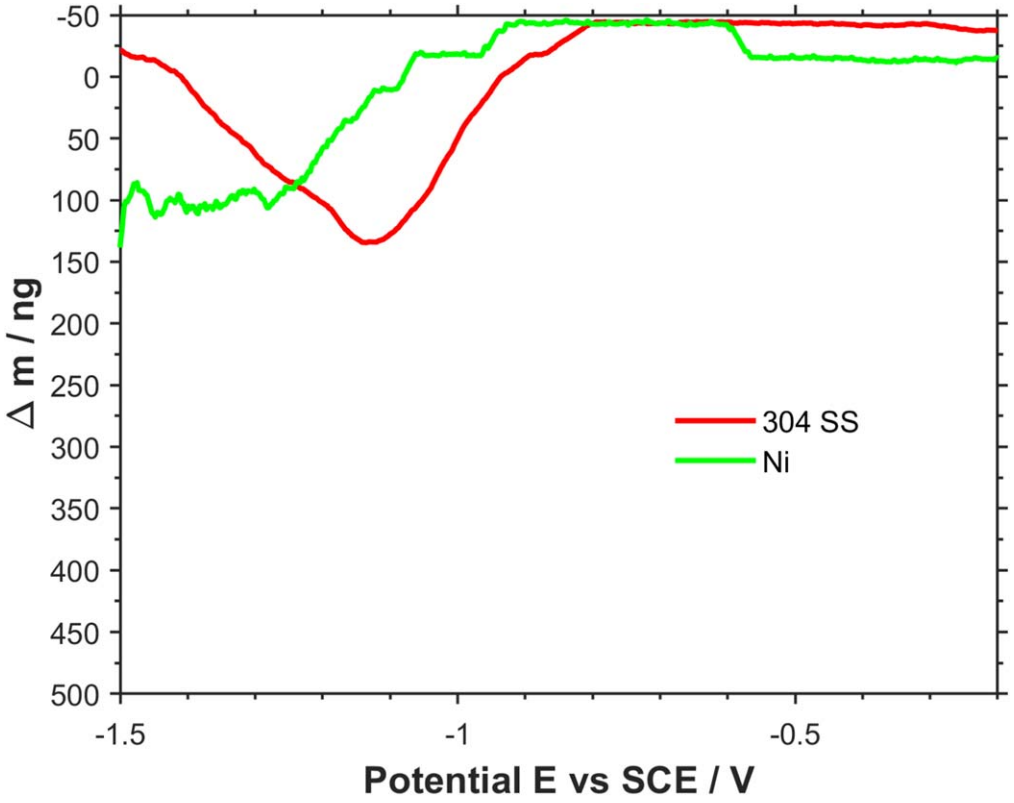

Figure 13. Mass change measured by the EQCM as a function of potential for 304 SS and Ni electrodes in a nickel-free solution containing 3.57 M KSO_3NH_2 and 0.65 M $B(OH)_3$.

position of the hydrogen peak to a less negative potential, rather than change its magnitude. This effect mainly arises from the −59 mV per pH unit shift in reversible potential of the HER for H^+ or H_2O reduction. For the less well buffered system (e.g. 0.49 M $B(OH)_3$) the interfacial pH is higher so that the onset of HER occurs at more negative potential, and there will be kinetic contributions too. Importantly, despite the significant hydrogen partial current reducing overall current efficiencies, the interfacial pH does not increase enough to cause $Ni(OH)_2$ to form. This arises due to the solution buffering by polyborates or nickel-borate species.

Regarding the proton donation model[18] where various borate and polyborate species minimises interfacial pH rises by delaying the transition to H_2O reduction, the current experimental results offer some limited support for this in the low current density regions. For example, the data in Figs. 9–11 show that, at the two highest $B(OH)_3$ concentrations and for current densities below 2 mA cm^{-2}, there is an initial period when the current efficiency is very low. This is consistent with Zech's suggestion[18] that polyborates or nickel borate complexes are operating as proton donors so that the limiting current density for H^+ reduction is increased from its nominal value of 1 mA cm^{-2} at pH = 3. This initially enhances H^+ reduction and lowers the current efficiency but, as the current density is increased, the reduction of nickel ions and H_2O dominates, and higher current efficiencies are achieved (Fig. 11). Zech's modelling study[18] indicates that the limiting current can only be enhanced by a factor of 2–5 times by this mechanism, and beyond this limit H_2O reduction is significant and the interfacial pH will invariably increase. The suppression of $Ni(OH)_2$ formation observed at high current densities (e.g. 10–50 mA cm^{-2}) in this study must therefore arise from conventional buffering and/or suppression of the H_2O reduction reaction.

As noted in the introductory section, one proposed model for the action of boric acid is its adsorption on the surface where it could block reaction sites for either the HER involving H^+ or H_2O or nickel deposition. There is some indirect evidence for this in studies of the H^+ reduction reaction in sulfate and sulfamate solutions, where the limiting current is reduced at higher boric acid concentrations. This is attributed to a decrease in the active area arising from $B(OH)_3$ adsorption and has mostly been reported[17,18,23,24,33] at low currents where H^+ reduction occurs, and where the electrode potential is at a value which favours boric acid adsorption. However, suppression of the HER at higher current densities where H_2O reduction dominates has also been reported,[5,7] and this has also been attributed to the adsorption of $B(OH)_3$. In a study of Ni deposition from a Watts bath, the authors[5] proposed pH buffering due to a Ni-borate complex at low current densities, and suppression of the HER at higher values.

Some earlier studies have shown the boric acid can absorb on Ag[59] and Pt[60] electrodes in acidic and neutral media. For example, the adsorption of $B(OH)_3$ has been reported at a potential, $E > +0.3$ V vs SCE in 0.1 M $HClO_4$ on Pt.[60] Note that, as boric acid is a neutral and relatively small molecule, its maximum absorption should occur at the potential of zero charge (pzc). For electrodes such as Ni and Fe in sulfamate or sulfate electrolytes the pzc would typically occur at $E_{pzc} \approx -0.40$ V vs SCE,[61,62] and this corresponds more to the region where H^+ reduction occurs. At more negative potentials $B(OH)_3$ would tend to desorb and it is less probable that it would be a significant adsorbed species at potentials of $E < -1.0$ V. Other polyborate and monoborate species (Table I) and the sulfamate ion are negatively charged and are therefore even less likely to absorb at potentials negative of the pzc.

Given its possible importance, EQCM data obtained in nickel-free sulfamate solution containing 3.57 M KSO_3NH_2 and 0.65 M $B(OH)_3$ was analysed to see if there was a mass increase that could be attributed to the adsorption of boric acid (Fig. 13). Note that the absorption of one monolayer of boric acid would correspond to an EQCM mass change of 80 ng assuming a packing density of 4.0×10^{15} molecules cm^{-2}. As only hydrogen is evolved, there should be a negligible mass change but there is a significant increase that starts at a potential of −0.90 V and peaks at −1.2 V vs SCE

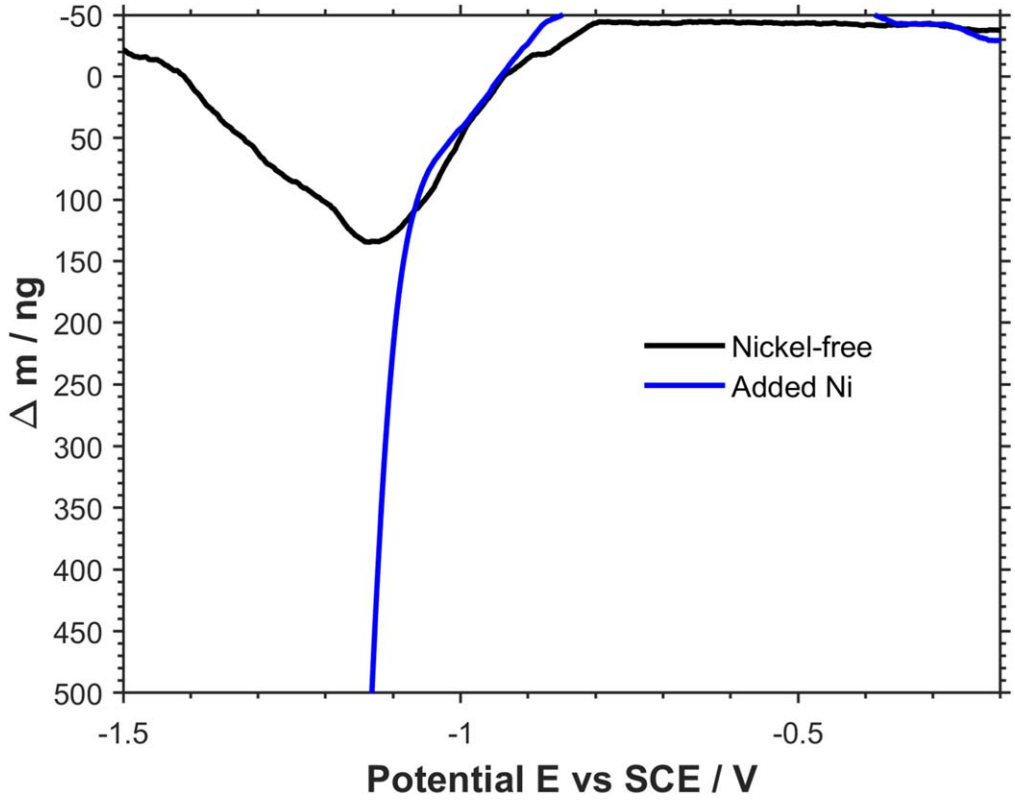

Figure 14. Mass change measured by the EQCM as a function of potential for 304 SS electrodes in a nickel-free 3.57 M KSO_3NH_2 and 0.65 M $B(OH)_3$ electrolyte and one to which 0.018 M $Ni(SO_3NH_2)_2$ was added.

($\Delta m \approx 150$ ng). Thereafter, the species desorbs and is fully desorbed by the time that potential reaches −1.40 V. These experiments were also repeated on a nickel coated crystal, which might more readily represent the substrate under electroforming conditions. This showed a similar mass gain feature ($\Delta m \approx 100$ ng) starting at a potential of −0.95 V vs SCE and extending to −1.5 V. These cannot be attributed to nickel borate complexes and the absorption of negatively charged mono and polyborate species is less favoured than neutral boric acid. Figure 13 therefore suggests that boric acid is forming an adsorbed blocking layer in the potential region where H_2O reduction is expected to occur.

In order to examine the relationship between Ni deposition and boric acid absorption, an EQCM experiment employing a 304 SS substrate was performed in a dilute nickel solution containing 0.018 M $Ni(SO_3NH_2)_2$ (i.e. 1% of the standard concentration) 3.57 M KSO_3NH_2 and 0.65 M $B(OH)_3$. Figure 14 shows that a similar absorption feature develops at −0.90 V vs SCE, but at a potential of −1.1 V the mass increases rapidly due the deposition of nickel. Note that the onset of nickel deposition is shifted from that observed (−0.95 V) in more concentrated solutions (Figs. 9 and 12) and this is due to a combination of the reversible potential shifting by −0.06 V and also kinetic effects. Therefore, Fig. 14 does not indicate that boric acid absorption precedes Ni deposition in more concentrated solution, but it does show that adsorption still occurs in the presence of nickel species.

Assuming the mass changes shown in Fig. 13 arise due to boric acid adsorption, this would correspond to the formation of approximately one or two monolayers of $B(OH)_3$. These absorptions occur at more negative potentials than the nominal pzc, however, Bockris[63] has noted that it is not uncommon for the maximum adsorption of neutral species to occur at potentials that are substantially more negative than the nominal pzc. As a relevant example, in the electrodeposition of CoFe alloys from sulfate electrolytes, the maximum absorption of neutral saccharin molecules occurred at $E = -1.35$ V vs SCE compared to $E_{pzc} \approx -0.5$ V.[64] Similarly, n-decylamine adsorption on copper and nickel electrodes was observed to be at a maximum at potentials that were −0.3 V to −0.7 V more cathodic than the estimated pzc for these metals.[65]

Even though the nature of the adsorbed species cannot be assigned unambiguously it is clear from a comparison of Figs. 12 and 13, both of which contain 0.65 M $B(OH)_3$, that it strongly influences the partial current for the HER. The hydrogen partial current starts to increase at −0.85 V but reaches a maximum at −0.95 V and then starts to decline. This corresponds closely to the potential region where $B(OH)_3$ adsorption commences and then attains its maximum value (Fig. 13). Therefore, the observed suppression of the H_2O reduction (Fig. 12) appears largely due to the adsorption of the boric acid species, but this has a minimal effect on nickel deposition. This finding agrees with some earlier studies[5,7,17,18,23,24,33] which proposed that boric acid suppresses the HER arising from H^+ or H_2O reduction. This inhibition of the HER assists in minimising pH rises at high current densities, and operates in concert with normal solution buffering arising from polyborates and nickel borate species.

Conclusions

This study has examined the role of boric acid in nickel electroforming from sulfamate electrolytes using a combination of speciation modelling and electrochemical studies employing an EQCM. While it is clear from prior literature that the main function of boric acid additions is to minimise interfacial pH changes, the means by which this is achieved is still disputed. Various models have been developed to explain the action of boric acid and these typically involve pH buffering effects associated with monoborate, polyborate or nickel borate species. Solution modelling has indicated that buffering by triborate or nickel borate species is likely to be responsible for this effect, and the buffer capacity is enhanced as the pH and boric acid concentration increase. However, the possibility that nickel-borate complexes are the main electroactive species was

discounted as the speciation analysis indicated that under typical electroforming conditions their concentration is <1% that of uncomplexed nickel ions. Only for pH > 5.5 do the nickel-borate complexes become more important, but the electroforming solutions precipitate at pH = 6 preventing them from achieving a significant concentration.

While the speciation modelling excluded some proposed models for the action of boric acid, electrochemical measurements were required to evaluate the remaining models. Polarisation and EQCM data indicated that, without added boric acid, electrodeposits typically contained $Ni(OH)_2$, while boric acid additions prevented this and allowed Ni to be deposited with a current efficiency approaching unity. Boric additions were found to have a significant influence on the partial current densities for nickel and hydrogen, and therefore on the current efficiency. In general, nickel deposition was enhanced by boric acid additions while the HER was strongly inhibited at certain potentials. Some evidence was found for polyborate or nickel borate complexes acting as proton donors, but this effect was only relevant at low current densities and high boric acid concentrations.

In nickel-free sulfamate solutions it was observed that a species, most probably boric acid, adsorbed on the surface and this occurred at potentials that corresponded to the suppression of H_2O reduction observed in the nickel-containing electroforming solutions. It therefore appears likely that the control of interfacial pH arises principally from two complementary sources. Firstly, there is conventional pH buffering due to the formation of polyborate and nickel-borate species in the solution and, secondly, inhibition of the H_2O reduction reaction by an adsorbed species. In combination, these two effects facilitate the electroforming of nickel deposits whose properties are not compromised by the incorporation of oxides or hydroxides inclusions.

ORCID

C. Enowmbi Tambe https://orcid.org/0000-0002-1257-6213
T. A. Green https://orcid.org/0000-0002-3538-5217

References

1. M. Schlesinger and M. Paunovic, *Modern Electroplating* (Wiley, New York) 5th ed. (2010).
2. W. E. G. Hansal, *Galvanotechnik*, **110**, 881 (2019).
3. https://echa.europa.eu/registry-of-svhc-intentions/-/dislist/details/0b0236e180e4b39c.
4. https://echa.europa.eu/documents/10162/aefd785e-1679-7337-75d4-54345f11165e.
5. Y. Tsuru, R. Takamatsu, and K. Hosokawa, *J. Surf. Finish. Soc. Jpn*, **44**, 39 (1993).
6. Y. Tsuru, M. Nomura, and F. R. Foulkes, *J. Appl. Electrochem.*, **32**, 629 (2002).
7. K. Fukuda, Y. Kashiwa, S. Oue, T. Takasu, and H. Nakano, *ISIJ Int.*, **61**, 919 (2021).
8. A. Vicenzo and P. L. Cavallotti, *Russ. J. Electrochem.*, **44**, 716 (2008).
9. S. H. Goods, J. J. Kelly, A. A. Talin, J. R. Michael, and R. M. Watson, *J. Electrochem. Soc.*, **153**, C325 (2006).
10. M. Motoyama, Y. Fukunaka, T. Sakka, and Y. H. Ogata, *J. Electrochem. Soc.*, **153**, C502 (2006).
11. J. J. Kelly, S. H. Goods, A. A. Talin, and J. T. Hachman, *J. Electrochem. Soc.*, **153**, C318 (2006).
12. A. H. DuRose, *Plat. Surf. Fin.*, **64**, 52 (1977).
13. E. B. Saubestre, *Plating*, **45**, 927 (1958).
14. B. V. Tilak, A. S. Gendron, and M. A. Mosoiu, *J. Appl. Electrochem.*, **7**, 495 (1977).
15. J. P. Hoare, *J. Electrochem. Soc.*, **133**, 2491 (1986).
16. J. P. Hoare, *J. Electrochem. Soc.*, **134**, 3102 (1987).
17. J. Horkans, *J. Electrochem. Soc.*, **126**, 1861 (1979).
18. N. Zech and D. Landolt, *Electrochim. Acta*, **45**, 3461 (2000).
19. M. Watanabe, Y. Wakuda, Y. Nakamaru, K. Tashiro, and H. Honma, *J. Surf. Finish. Soc. Jpn*, **58**, 317 (2007).
20. H. Riechmann, M. Muller, and A. Meyerovich, *Trans. IMF*, **95**, 73 (2017).
21. https://aalberts-st.com/people-culture/news/boric-acid-free-nickel-plating/.
22. J. Ji, W. C. Cooper, D. B. Dreisinger, and E. Peters, *J. Appl. Electrochem.*, **25**, 642 (1995).
23. H. Deligianni and L. T. Romankiw, *IBM. J. Res. Develop.*, **37**, 85 (1993).
24. M. A. Rigsby, T. A. Spurlin, and J. D. Reid, *J. Electrochem. Soc.*, **167**, 112507 (2020).
25. J. Ji and W. C. Cooper, *Electrochim. Acta*, **41**, 1549 (1996).
26. R. E. Mesmer, cf Baes, and F. H. Sweeton, *Inorg. Chem.*, **11**, 537 (1972).
27. R. L. Bassett, *Geochim. Cosmochim. Acta*, **44**, 1151 (1980).
28. L. M. S. G. A. Applegarth, C. C. Pye, J. S. Cox, and P. R. Tremaine, *Ind. Eng. Chem. Res.*, **56**, 13983 (2017).
29. G. N. Mukherjee and A. Das, *J. Indian Chem. Soc.*, **79**, 45 (2002).
30. A. Bousher, *J. Coord. Chem.*, **34**, 1 (1995).
31. A. Graff, E. Barrez, P. Baranek, M. Bachet, and P. Benezeth, *J. Solution Chem.*, **46**, 25 (2017).
32. A. Lachenwitzer and O. M. Magnussen, *J. Phys. Chem. B*, **104**, 7424 (2000).
33. A. Hankin, "Electrochemical recovery of nickel from nickel sulfamate plating effluents." *PhD Thesis*, Imperial College (2012).
34. S. Roy and E. Andreou, *Curr. Opin. Electrochem.*, **20**, 108 (2020).
35. E. Andreou and S. Roy, *Front. Chem. Eng.*, **4**, 755725 (2022).
36. J. A. McGeough, M. C. Leu, K. P. Rajurkar, A. K. M. De Silva, and Q. Liu, *CIRP Ann.*, **50**, 499 (2001).
37. S. A. Watson, *Trans. IMF*, **77**, 10 (1999).
38. N. Pewnim and S. Roy, *J. Electrochem. Soc.*, **162**, D360 (2015).
39. T. A. Green, C. E. Tambe, and S. Roy, *J. Electrochem. Soc.*, **169**, 092510 (2022).
40. T. A. Green, A. E. Russell, and S. Roy, *J. Electrochem. Soc.*, **145**, 875 (1998).
41. S. Roy, *Surf. Coat. Technol.*, **105**, 202 (1998).
42. T. A. Green and S. Roy, *J. Electrochem. Soc.*, **153**, C157 (2006).
43. H. Gamsjager, J. Bugajski, T. Gajda, R. Lemire, and W. Pries, *Chemical Thermodynamics of Nickel* (Nuclear Energy Agency, OECD Publishing, Paris) (2020).
44. JESS (Joint Expert Speciation System) Thermodynamic Database (version 8.9) https://doi.org/10.5281/zenodo.7700023.
45. NIST Critically Selected Stability Constants of Metal Complexes: Version 8.0 (2013).
46. L. D. Petit and K. J. Powell, *The IUPAC Stability Constant Database (SC-Database) version 4.71* (Academic Software, U.K.) (2005).
47. D. Golodnitsky, N. V. Gudin, and G. A. Volyanuk, *J. Electrochem. Soc.*, **147**, 4156 (2000).
48. T. Raynaud, M. Bachet, P. Benezeth, and A. Graff, *J. Solution Chem.*, **53**, 1017 (2024).
49. I. Tabakovic, S. Rieimer, R. Kvitek, P. Jallen, and V. Inturi, *Magnetic Materials, Processes and Devices VI*, ed. S. Krongelb et al. (The Electrochemical Society Proceeding Series, Pennington, NJ) (2001).
50. J. Vazquez-Arenas and M. Pritzker, *Electrochim. Acta*, **56**, 8023 (2011).
51. D. Gangasingh and J. B. Talbot, *J. Electrochem. Soc.*, **138**, 3605 (1991).
52. A. Hankin and G. H. Kelsall, *J. Appl. Electrochem.*, **42**, 629 (2012).
53. J. Vazquez-Arenas, L. Altamirano-Garcia, M. Pritzker, R. Luna-Sanchez, and R. Cabrera-Sierra, *J. Electrochem. Soc.*, **158**, D33 (2011).
54. J. Vanpaemal, M. H. van der Veen, C. Huyghebaert, S. De Gendt, and P. M. Vereecken, *ECS Trans.*, **50**, 29 (2013).
55. C. E. Davalos, J. R. Lopez, H. Ruiz, A. Mendez, R. Antano-Lopez, and G. Trejo, *Int. J. Electrochem. Sci.*, **8**, 9785 (2013).
56. K.-D. Song, K. B. Kim, S. H. Han, and H. K. Lee, *Electrochem. Comm.*, **5**, 460 (2003).
57. J. S. Santos, R. Matos, F. Trivinho-Strixino, and E. C. Pereira, *Electrochim. Acta*, **53**, 644 (2007).
58. V. P. Graciano, U. Bertocci, and G. R. Stafford, *J. Electrochem. Soc.*, **166**, D3246 (2019).
59. K. J. Stevenson, D. W. Hatchett, and H. S. White, *Langmuir*, **13**, 6824 (1997).
60. A. A. El-Shafei and A. Aramata, *J. Solid State Electrochem.*, **11**, 430 (2007).
61. E. McCafferty, *Introduction to Corrosion Science* (Springer, Berlin) (2010).
62. S. Trasatti and E. Lust, *Modern Aspects of Electrochemistry Vol. 33*, ed. R. E. White et al. (Springer, Boston) (2002).
63. J. O. 'M. Bockris and A. K. N. Reddy, *Modern Electrochemistry Vol. 2* (Plenum Press, New York) (1970).
64. S. R. Brankovic, *Electrochim. Acta*, **84**, 139 (2012).
65. J. O. 'M. Bockris and D. A. J. Swinkels, *J. Electrochem. Soc.*, **111**, 736 (1964).